Account

Chemical Vapor Deposition Polymerization of Poly(arylenevinylene)s and Applications to Nanoscience

Sung-Hoon Joo, Chun-Young Lee, Kyungkon Kim, Ki-Ryong Lee, and Jung-Il Jin[*]

Department of Chemistry and Center for Electro- and Photo- Responsive Molecules, Korea University, Seoul 136-701, Korea
[*]*E-mail: jijin@korea.ac.kr*
Received November 22, 2005

A review is made on the chemical vapor deposition polymerization (CVDP) of insoluble and infusible poly(arylenevinylene)s and its applications to nanoscience. Poly(*p*-phenylenevinylene) (PPV), poly(naphthylenevinylene)s, poly(2,5-thinenylenevinylene) (PTV), and other homologous polymers containing oligothiophenes could be prepared by the CVDP method in the form of films, tubes, and fibers of nano dimensions. They would be readily converted to graphitic carbons of different structures by thermal treatment. Field emission (FE) of carbonized PPV nanotubes, photoconductivity of carbonized PPV/PPV bilayer nanotubes and nanofilms also were studied.

Key Words : Chemical vapor deposition polymerization, Poly(arylenevinylene), Nano object, Field emission, Photoconductivity

Introduction

Preparation of insoluble and infusible polymers in desired shapes and dimensions is one of the most important challenges in synthetic polymer chemistry as the number of unprocessable polymers that are found to reveal attractive properties in electrical, optical, and photonics, increases in an unprecedented pace in recent years.[1-11] Polyacetylene, poly(*p*-phenylene),[9] poly(*p*-phenylenevinylene) (PPV),[10] polythiophene,[11] and poly(2,5-thienylenevinylene) (PTV)[6] are some of the representative examples. It, of course, is possible to modify the structures of the polymers to make them soluble: attachment of long alkoxy or alkyl substituents on the aromatic rings of the polymers and modification of the structure of aromatic rings to include heteroatoms are the most frequently utilized methods.[12-17] The methods, however, change not only the electronic and optical properties of the original polymers, but also thermal properties. In general, the alkyl and alkoxy groups reduce the thermal stability of the resulting polymers. The following polymers are representative substituted, soluble polyconjugated polymers, whose electrical, optical and fluorescence properties have been much studied.[12-22]
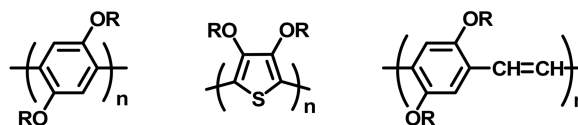

In this article, among many different classes of polyconjugated polymers, poly(arylenevinylene)s (PAVs) are the focus of our concern. The most widely used multistep synthetic procedure of PAVs through soluble precursors is the so-called Wessling-Zimmerman method[23,24]:
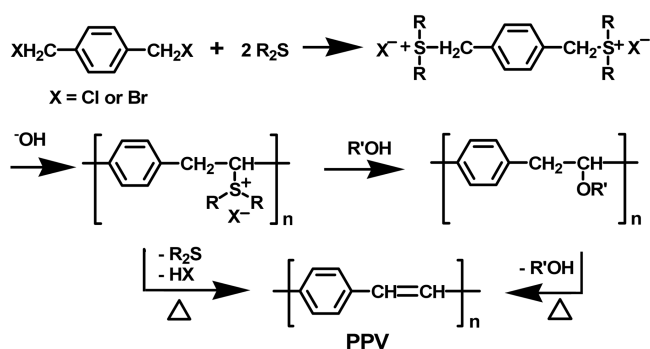
Jung-Il Jin received his B.S. (1964) and M.S. (1966) degrees from the Department of Chemistry, Seoul National University. In 1969, He earned his Ph. D. degree in physical chemistry (polymer chemistry) from the City University of New York. He has been a Professor at Korea University from 1974 to the present. He served as President of the Korean Chemical Society (2000) and the Polymer Society of Polymer (1997). He is now serving as the President (2006-2009) of the IUPAC Polymer Division. He received many awards including the Paul J. Flory Polymer Research Prize (2005), International Award of the Polymer Society, Japan (2004), King Saejong Memorial Award (1998), and Korea Science Award (1991). He is interested in liquid crystals, conducting polymers, PL and EL polymers, NLO polymers, nanostructured polyconjugated polymers, magnetic polymers, e-beam nanoprocessing, and materials science of DNA. He has published about 360 academic papers.

The above scheme shows two different possible precursor polymers, one is the water soluble sulfonium salt polymer and the other the organic soluble alkoxy polymer. The precursor polymers can be fabricated to desired shapes, which then are subjected to thermolysis to the final PPV polymer. The reaction mechanism of this reaction has been reviewed by Cho.[25] There are other synthetic routes by which PPV is prepared via soluble precursor polymers.[26-28]
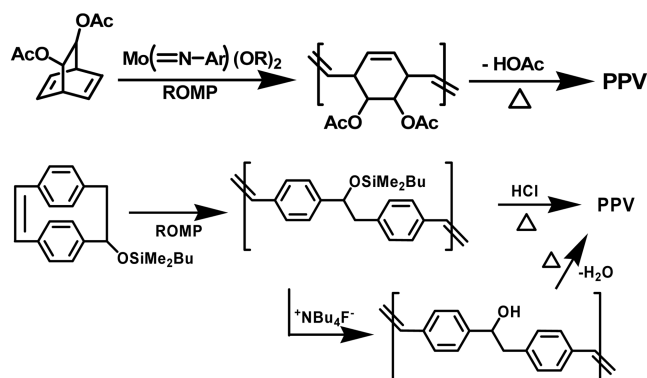

Both reactions rely on ring-opening metathesis polymerization (ROMP). A thorough review on the classical synthetic methods of PPV and related PAVs were made by Denton and Lahti.[29] All the precursor methods suffer from possible contamination of the final polymer with solvent, side products and catalyst residue.

About 10 years ago, a Philips research group reported that they could prepare thin films of PPV by the CVDP method and studied their electroluminescence properties.[30] A little bit later the Marburg (Germany) group performed a thorough structural analysis of the PPV films prepared by the same method.[31] In this new synthetic method, 1,4-bis(halomethyl)-benzenes are pyrolyzed in the gas phase to form a reactive intermediate, which undergoes an addition polymerization resulting in the formation of the precursor polymer. The precursor is subjected to dehydrochlorination to be converted to PPV.
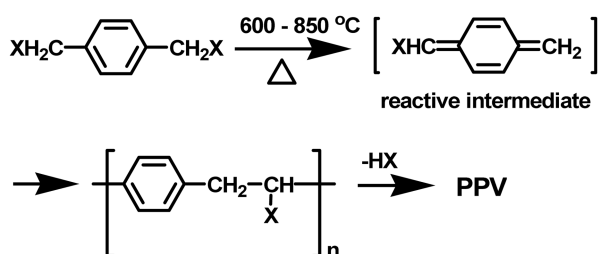
It should be noted that PPV can be prepared also by CVDP of dichlorocyclophane as reported earlier by Iwatsuki *et al.*[32]
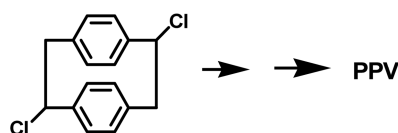
There are not yet many attempts in which the CVDP method is applied to the preparation of substituted PPVs.[33] Poly(p-xylene)(PPX) is synthesized by CVDP of p-xylene or paracyclophane.[34-39]
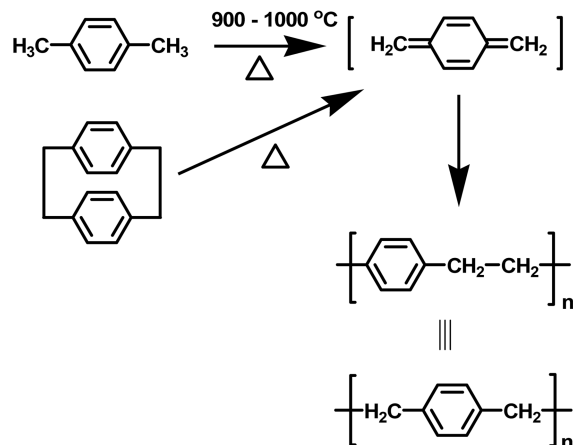
PPX is a crystalline polymer having high solvent resistance, low dielectric constant and excellent barrier properties. Due to its biocompatibility the polymers are of interest in medical applications. In fact, the CVDP method is most commonly used in the preparation of PPX, although the method can be utilized in the preparation of other polymers.[39]

Preparation of PPV Nano Objects. As alluded above, preparation of insoluble and infusible polyconjugated polymers in a desired dimension having an intended shape is impossible unless one has to go through a soluble precursor route. The self-assembly technique is the most popular method being employed for the construction of various shapes of organic and organometallic objects of nano dimensions.[40-45] This method belonging to the so-called 'bottom-up' approach, however, can not be readily applied to the insoluble polymers. On the other hand, the precursor polymers soluble either in water or in an organic solvent, can be coated on the surface of a substrate (flat, tubular, porous or spherical), and then they are subjected to the final treatment, usually thermolysis, resulting in the formation of nano shaped target polymers. In this method, the substrates act as templates. Therefore, the availability of proper templates is prerequisite in the soluble precursor approach. The CVDP method is resembles the later method, in which the surface of templates or substrates are utilized to accumulate polymer molecules. Figure 1 shows micrographs of PPV nano objects prepared by the CVDP method.

Recently, Jang *et al.*[46] could prepare polypyrrol nanotubes by the CVDP method on the inner surface of nanoporous anodic aluminum oxide(AAO) membrane template that was presoaked in an FeCl₃ aqueous solution. Evidently, deposited FeCl₃ catalyzes the polymerization of the pyrrol monomers in the gas phase. Electrochemical polymerization also is applicable to the preparation of nanotubes of some of the polyconjugated polymers.[47,48] One, of course, can prepare nanotubes of soluble polymers simply by soaking the
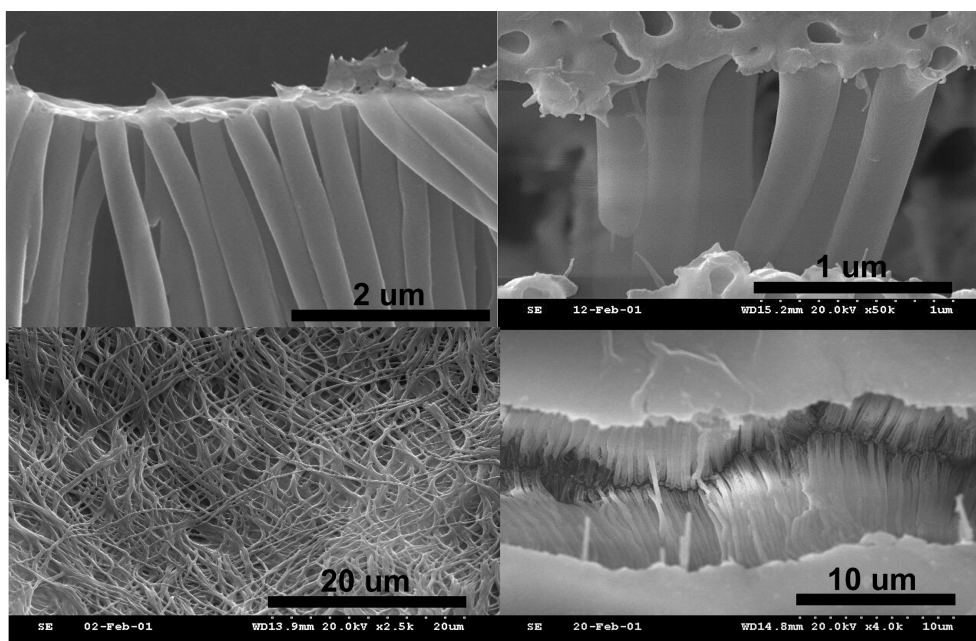
Figure 1. SEM images of PPV nano objects prepared by the CVDP method.[2]

nanoporous membranes or nano tubes in a solution of a polymer followed by evaporation of the solvent. Smith *et al.*[49] and Jang and Yoon[50] used inverse hexagonal emulsions as reaction vehicles for the preparation of PPV nano composites and polypyrrole nanotubes, respectively.

Polyaniline nanotubes and nanorods could be prepared by the self-assembly method in the presence of an inorganic acid dopant such as HCl and H_2SO_4.[51] Recently, interestingly, it was reported by Guo and coworkers[52] that well ordered poly(2-methoxy-5-(*n*-hexadecyloxy)-*p*-phenylenevinylene) nanotube could be easily prepared at the air/water interface by compressing the Langmuir-Blodgett films beyond the collapse point.

Among many advantages of the CVDP method the most important are i) easy synthetic process, ii) preparation of uncontaminated polymers, iii) convenient synthesis of insoluble polymers in desired nano shapes, iv) flexibility in the selection of substrates and templates, and v) smooth surface coverage. There also are several disadvantages in this method: i) the number of chemical reaction types usable is limited, ii) the monomer should be able to produce a thermally reactive intermediate in the gas phase, which implies that the variety of substituents one can attach to the main structure is limited, iii) the product yield is rather low (~30%), and iv) the study of the polymerization reactions is difficult when compared with conventional polymerization, and v) liberation of HX during polymerization can be harmful in electronic applications.

We[53] recently found that the CVDP of *p*-(methoxymethyl)-benzenyl chloride (MMBC) produces copolymers consisting of 1,4-phenylenevinylene (PV) and 1,4-phenyleneethanediyl (PE) units whose compositions vary continuously toward higher PE content as the monomer activation temperature is raised (Table 1).

Table 1. Composition of PAV copolymers prepared from *p*-(methoxymethyl)benzylchloride at different monomer activation temperatures[53]

Activation Temp. (°C)	PV unit[a] (mole %)	PE unit[b] (mole %)
650	52	48
700	35	65
750	31	69
800	26	74

[a]Phenylenevinylene unit. [b]Phenyleneethanediyl unit
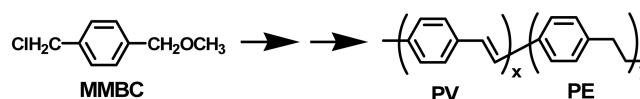
It is believed that much more of unsubstituted quino-dimethane intermediate is formed from the MMBC monomer than from 1,4-bis(chloromethyl)benzene at the pyrolysis temperatures. According to their UV-Vis absorption and photoluminescence (PL) spectra, the copolymers appear to be of random sequence.

Preparation of Other PAVs by CVDP Method. Application of the CVDP method could be successfully expanded to the preparation of a wide variety of poly(arylenevinylene)s whose chemical structures are shown below:

PT$_m$V (m = 1-4)   2,6- and 1,4-PNV   PAnV
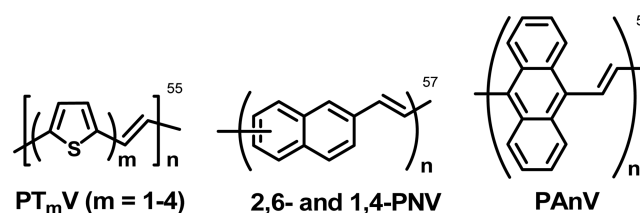
PT$_m$Vs are a series of polymers that contain an increased number of consecutively linked thienylene rings in the repeating unit. These polymers were prepared from the corresponding bis(chloromethyl) compounds.[54-56]
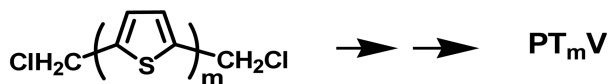
In the CVDP preparation of PT$_m$Vs, it was learned[55] that, in order to obtain good quality of polymer films, the monomer activation temperature has to be increased with increasing number (m) of the consecutively linked thienylene rings in the monomer.

As will be discussed in the next section, the content of the saturated unit also increased with increasing m owing to the elevated monomer activation temperature utilized. Figure 2 shows electromicrographs of nanotubes and nanorods of PTV prepared by CVDP using nanoporous alumina membranes as templates.

Poly(naphthylenevinylene)s also could be prepared via CVDP from the bis(chloromethyl) monomers.[57] Surprisingly, poly(9,10-anthracenediylvinylene) (PAnV) could not be prepared by conventional methods.[58] We[57], however, could prepare the same polymer by the CVDP method.

Chemical Structures of PAVs Prepared by CVDP. The chemistry involved in the CVDP polymerization of PPV is much more complicated than as discussed by the Marburg

group and more in detail by Vaeth and Jensen.[59-61] The final PPV samples prepared by the CVDP of bis(1,4-halomethyl)-benzene contain a low-level of the saturated 1,4-phenylene-ethanediyl (PE) units in addition to the unsaturated 1,4-phenylenevinylene (PV) units.
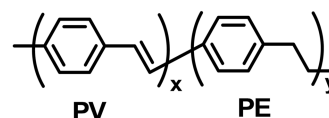

Figure 3 shows the IR spectrum of the final PPV in the wave number (cm^{-1}) region where C-H stretching vibration modes absorb. As indicated in the spectrum saturated C-H stretching absorptions are observed at 2858 and 2915 cm^{-1} in addition to the absorption at 3024 cm^{-1} for the unsaturated C-H stretching mode. This suggests us that quinodimethane is formed together with quinohalodimethane upon pyrolyzing the monomer:
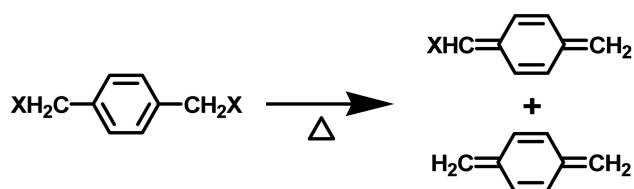
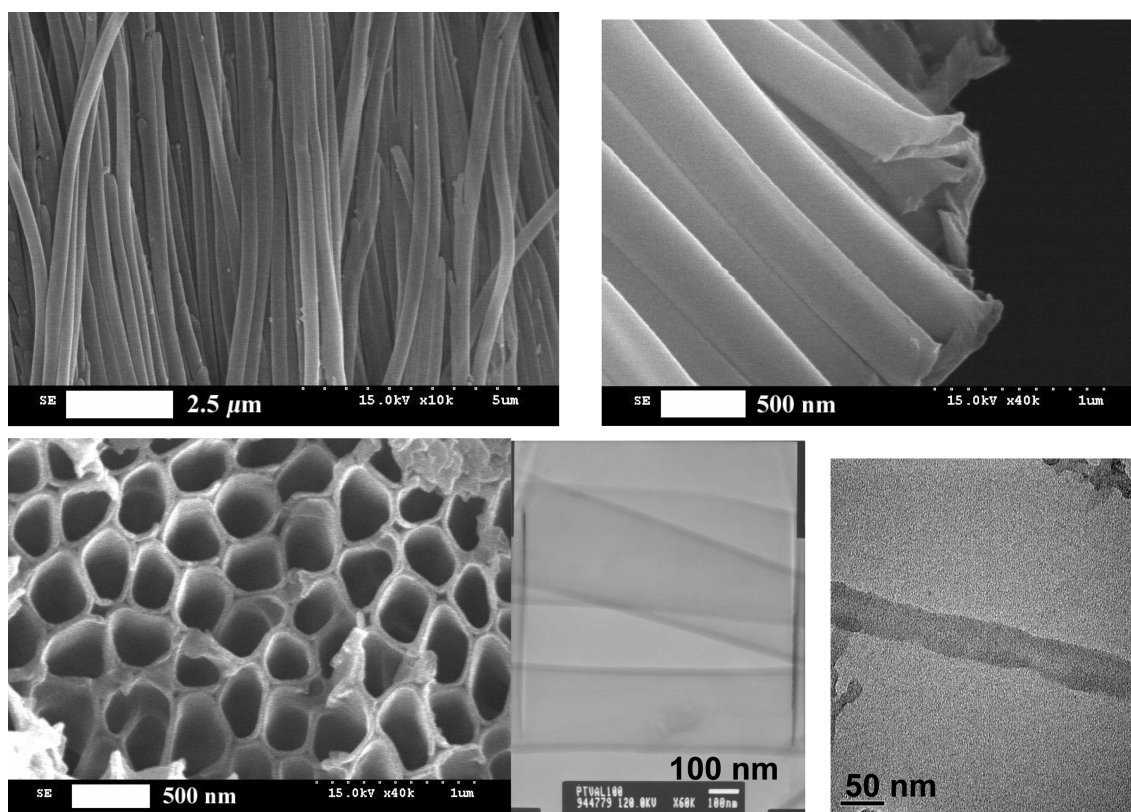According to the Marburg group's report,[31] the use of gem-

Figure 2. SEM and TEM images of nanotubes and a nanorode of PTV prepared by CVDP using nanoporous alumina membranes as templates.[54]
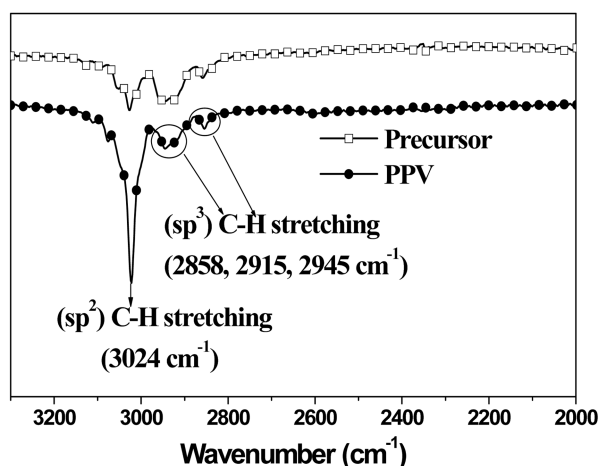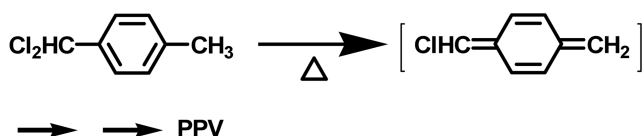
Figure 3. IR spectra of the precursor and final PPV nanotubes.[69]

dihalo-*p*-xylene in CVDP produces PPV containing no saturated unit. Evidently, in this case, there is no possibility for the unsubstituted quinodimethane to form:

There is another point to be noted in the structure of PPVs obtained by CVDP. For example, in the formation of PPV two different modes of addition are possible for the reactive intermediate, chloroquinodimethane : head-to-tail and head-to-head reactions.
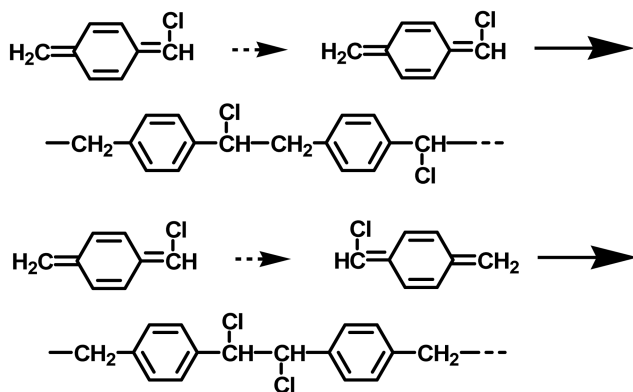
Although the head-to-tail addition should be preferable, the formation of the head-to-head (hence, tail-to-tail) structure can not be completely excluded. In other words, irregularities in the mode of addition of the reactive intermediates are possible. These irregularities also can cause the formation of the saturated units along the chain. Experimental proof for this possibility, however, has to be further studied.

Figure 4 compares the IR spectra of the $PT_mV(m=1-4)$ series prepared by CVDP.[55] The stretching absorption of C=C bonds in the thiophene ring appears at 1450 cm^{-1} and the thiophene overtone bands are observed at 1500-1750 cm^{-1}. There are several points worthy of special attention.

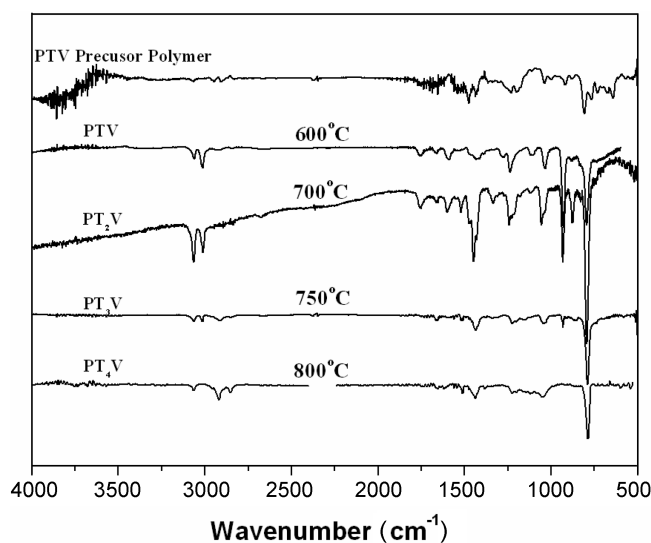**Figure 4**. IR spectra of PT_mV films. The temperature indicates monomer activation temperature.[54,55]

All the spectra commonly show sp^3 C–H stretching absorption at about 2910 cm^{-1} in addition to the sp^2 =C–H stretching mode at 3010 cm^{-1}. The relative intensity of the saturated sp^3 C–H stretching mode increases with increasing number of the thienylene rings in the repeating unit. At the same time, the intensity of the absorption peak at 930 cm^{-1} for the trans vinylene =C–H out-of-plane bending mode diminishes with increasing m, which is due to the progressively reduced proportion of the vinylene group in the repeating unit with increasing m. This can be ascribed to two different factors: monomer activation temperature and relative stability or easy of formation of the two reactive intermediates. As indicated in the figure, the monomer activation was performed at elevated temperatures to obtain polymer thin films of satisfactory quality. This would lead to the formation of higher amount of unchlorinated intermediates that produce saturated structural unit.
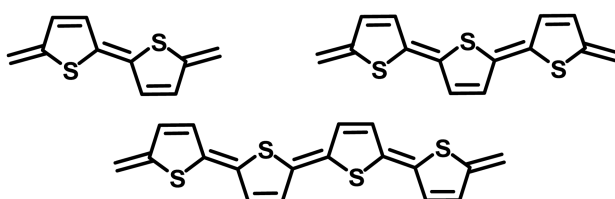

Moreover, as the number of consecutively linked thienylene rings increases, most probably the difference in the thermodynamic stability and also in the rate of formation of unsubstituted and chlorine-substituted intermediates is expected to decrease.
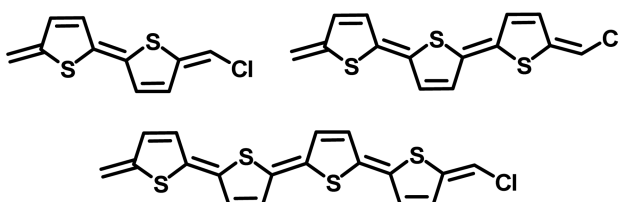
However, direct experimental evidence for this supposition is lacking at the present time.

We[57] tried CVDP of 1,4-, 1,5-, 2,6-, and 1,8-bis(chloromethyl)naphthalenes and found that 1,4-, 1,5- and 2,6-isomers produce the corresponding poly(naphthylenevinylene)s, respectively, but the 1,8-isomer failed in doing so. This difference is ascribed to the ability or inability to form the reactive intermediate:
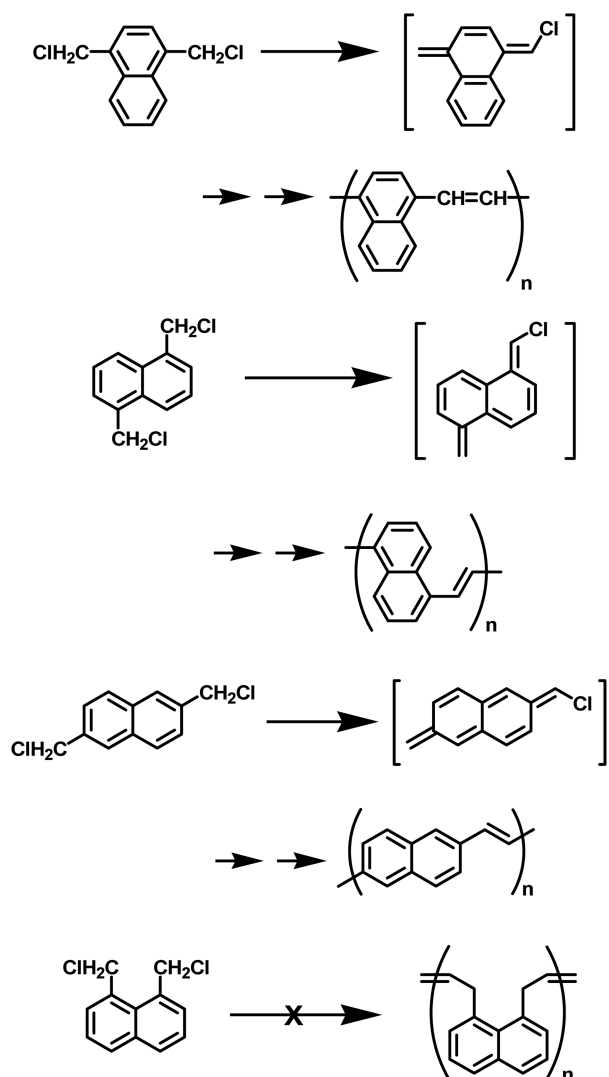
Differently from its isomers, evidently, 1,8-bis(chloromethyl)naphthalene is not able to form any π-conjugated intermediate. Therefore, the isomer is not able to produce the corresponding vinylene polymer by CVDP.

As in the case of PPV and PT$_m$Vs, poly(naphthylenevinylen)s prepared by the present CVDP method also contain saturated units in addition to the major unsaturated units again indicating that unchlorinated intermediates are formed together with chlorinated intermediates when the monomers were pyrolyzed at high temperatures. It also is possible that head-to-head addition between the chlorinated intermediates occurs to a certain extent.
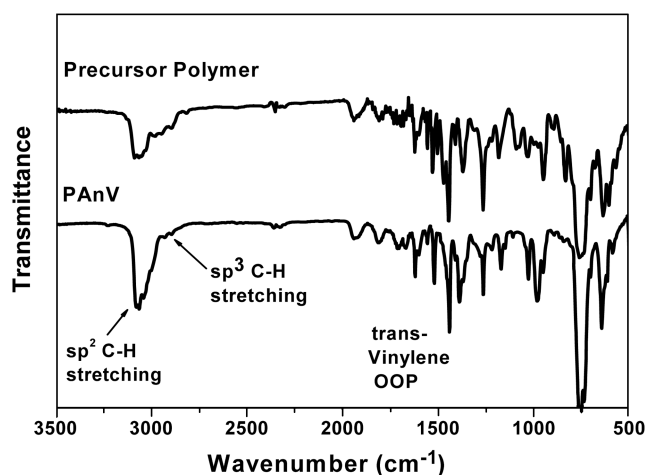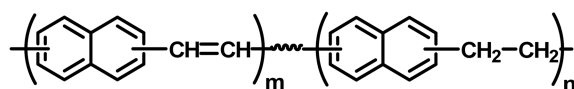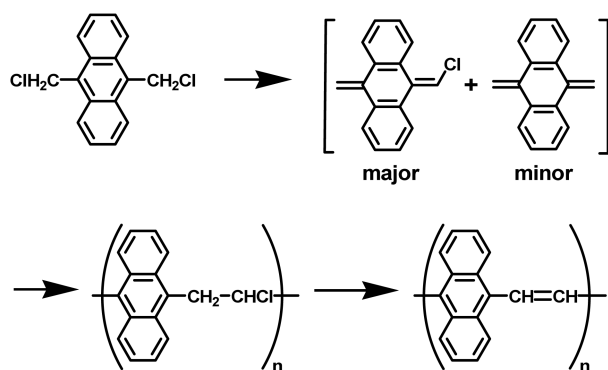

Figure 5. IR spectra of the precursor and final PAnV.[57]

Müllen *et al.*[58] tried to prepare poly(9,10-anthracenediyl-1,2-ethenediyl) [poly(9,10-anthracenyl vinylene): PAnV] in solution utilizing many different synthetic methods, but only in vain. We[57] became curious if the CVDP method could be applied to the preparation of PAnV. The bis(chloromethyl) monomer was pyrolyzed at 250 °C and the precursor polymer was collected on a substrate at room temperature. The precursor was converted to the final polymer by thermal treatment at 300 °C. Figure 5 compares the IR spectra of the precursor and final polymers. The most outstanding changes noticed are that a new sharp peak appears at 980 cm^{-1} in the IR spectrum of the final polymer, which is due to trans vinylene =C$-$H out-of-plane bending. At the same time the intensity of the peaks at about 2900 cm^{-1} (sp^3 C-H stretching vibration mode) was significantly reduced, although it didn't completely disappear.

The ^{13}C CP-MAS NMR spectrum of the final polymer is given in Figure 6 which exhibits resonance peaks for sp^2 carbons at 115-135 ppm, sp^3 C-Cl carbons at 67 ppm and sp^3 C-H carbons at 25 ppm. The peak intensity of sp^3 C-Cl and C-H carbons is much weaker than those of sp^2 carbons. The spectrum basically coincides with the structure anticipated, but it is evident that the final polymer again contains a minor proportion of saturated structures. Thermogravimetric analysis of the precursor showed that 15 wt% loss occurred at 150-300 °C that agrees well with the calculated value (15.3%). Therefore, it is our belief that the CVDP method, for the first time, could be successfully used in the preparation of poly(9,10-anthracenylvinylene).

Dependence of Morphology of PPV Thin Films on the Nature of Substrate. The CVDP method requires the use of a substrate. This raises a question if the nature of the surface of a substrate would influence the morphology of polymers obtained by CVDP. We[62] studied crystallinity and chain orientation of PPV formed on the surface of quartz, amorph-

Figure 6. ^{13}C CP-MAS NMR spectrum of PAnV.[57]

ous and (001) and (111) crystalline silicons.

Figure 7 compares the wide-angle X-ray diffractograms of PPV films obtained on different surfaces. Surprisingly, PPV films obtained on the Si (001) and (111) surfaces are semi-crystalline (Figure 7a and 7b), whereas those obtained on the amorphous silicon and quartz surfaces are either very low in crystallinity (Figure 7d) or almost amorphous (Figure 7c). This indicates that crystalline surfaces favor the formation of crystalline PPV, whose lattice parameters match fair well with those reported earlier by Chen *et al.*[61] They claimed that stretched PPV films have a crystallinity of the herring-bone type with p2gg symmetry. We, however, do not find any lattice matching between the lattices of PPV crystal structure formed and the crystalline silicon substrates. The mechanism for the surface control of PPV morphology requires further studies.

We[62] and Vaeth and Jensen[59] also learned from the IR reflection absorption spectroscopy (IRRAS) that PPV chains, when prepared on appropriate surfaces, can be induced to orient. When we performed CVDP of PPV on the (001) surface of silicon, the IRRAS of the PPV film exhibited a stronger dependence of the out-of-plane (oop) bending

modes of phenyl C-H and trans vinylene C-H on the incident angle of the *p*-polarized IR beam. The intensity of the oop bending absorption bands is minimum at the incident angle of 60°, which indicates that the PPV chains are inclined about 60° to the surface of the Si wafer substrate. In contrast, the PPV film prepared on the quartz surface did not reveal such a dependence on the incident angle. This again implies that PPV chains in this case are much more randomly oriented.

In addition, the studies on the dependence of polarized fluorescence (Figure 8) and UV-vis absorption (Figure 9) properties[62] of the PPV films prepared on the Si(001) surface confirmed that polymer chains are oriented and slanted about 30° to the substrate surface. The spontaneous orienta-tion of the polymer chains provides an interesting fabricating method for the preparation of chain-oriented polymer films

Figure 7. X-ray diffractograms of precursor and PPV films grown on the surface of (a) Si (001) wafer, (b) Si (111) wafer, (c) amorphous silicon, and (d) quartz.[62]

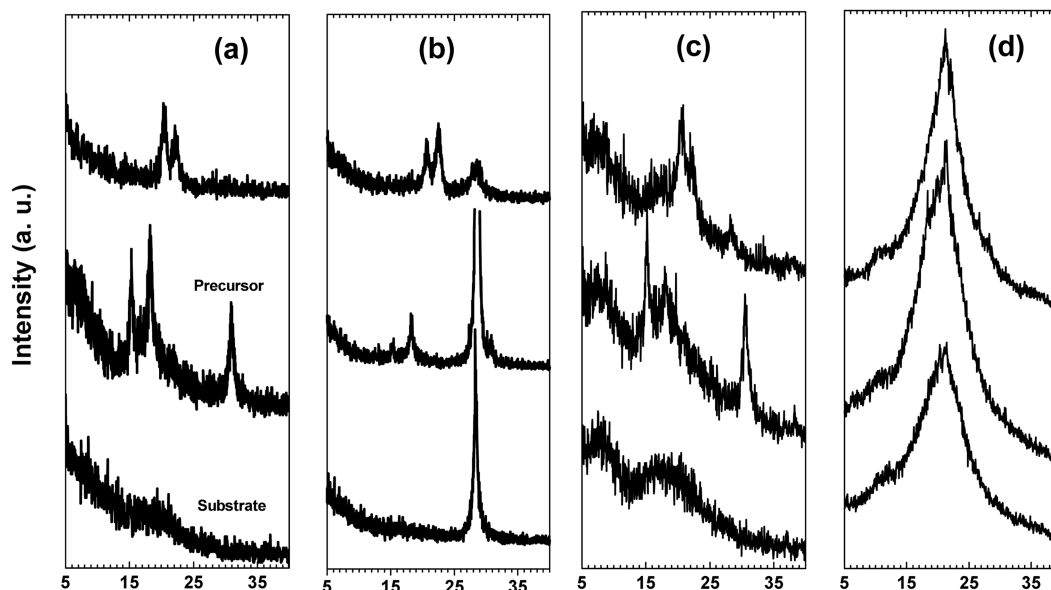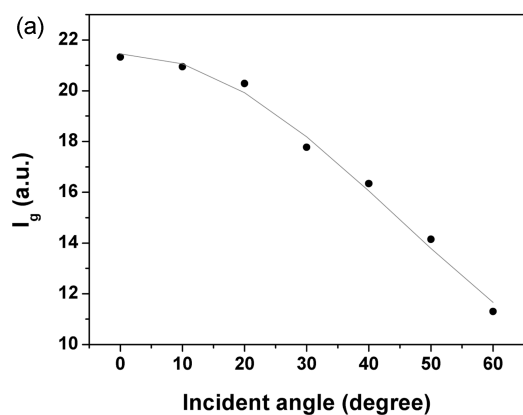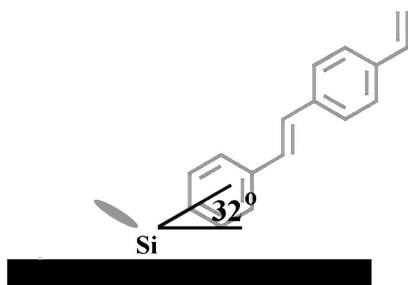**Figure 8.** (a) Generated fluorescence intensity I_g of PPV on crystalline silicon (dot) and least square fitted data (line) and (b) proposed structure of PPV on the Si wafer (001) surface.[62]

with the CVDP method. Coincidentally, this angle is about the same as the bond angle expected when there are direct Si-C bonds between the wafer Si atoms and CH_2-ends of PPV chains. Although there is a genuine possibility for a reaction between the wafer surface and reactive intermediates of CVDP, evidence of the direct chemical bonding is lacking at the present moment.

An indirect evidence, however, could be provided by running CVDP of PPV on the surface of liquid polysiloxane containing Si-H group.
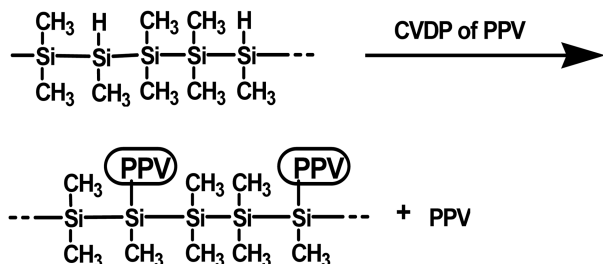
Even after the final mixture was subjected to Soxhlet extraction in methanol that is a good solvent for the starting polysiloxane, the residue contained a substantial amount of polysiloxane moiety as shown by the IR spectrum in Figure 10.[63] Moreover, the original absorption intensity of the -Si-H stretching mode was reduced to almost none, suggesting involvement of the -Si-H group in reactions during polymerization with reactive intermediates formed from the
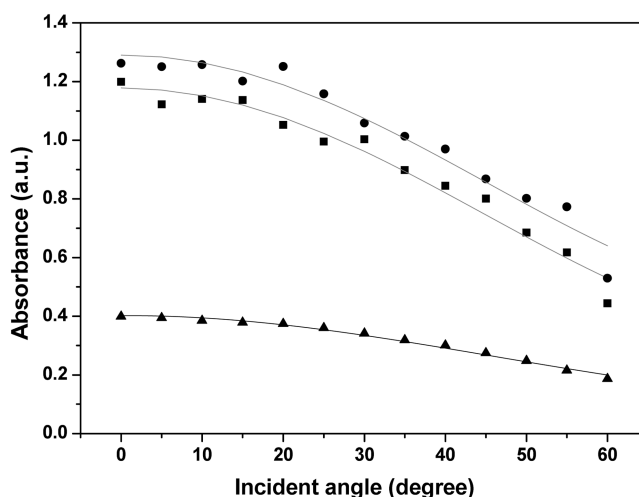
Figure 9. The UV-vis absorbance data at the wave length of 427 nm (●), 430 nm (■), 480 nm (▲) and least square fitted data. The slant angles φ_s of PPV on crystalline silicon sample were 30°, 27°, and 30°, respectively.[62]
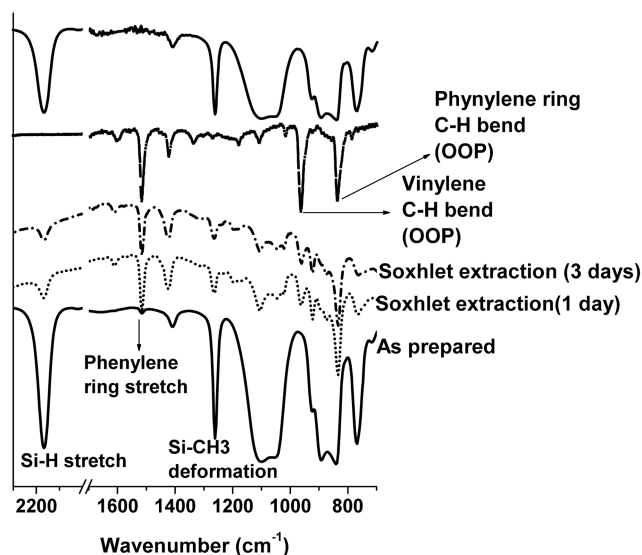
Figure 10. IR spectra of PPV prepared on polydimethylsiloxane by CVDP.[63]

thermolysis of the monomer.

Surface control of morphology of the polymers formed on a specific substrate appears to depend on the monomers utilized in CVDP. For example, PTV films obtained on the Si(001) surface was amorphous (Figure 11), which is in a great contrast to the PPV case. However, PT_2V and PT_3V thin films obtained even on the SiO_2 surface are crystalline (Figure 11). These observations lead us to the conclusion that not only the nature of a surface but also the structure of the polymer backbone controls the morphology of the polymer thin films obtained by the CVDP method. This field requires much more studies before one can draw more, definitive correlation between the surface control of polymer morphology and chemical structure of polymers.

Luminescence Properties of Nano PPVs. Figure 12 contains UV-vis and photoluminescence(PL) spectra of PPV
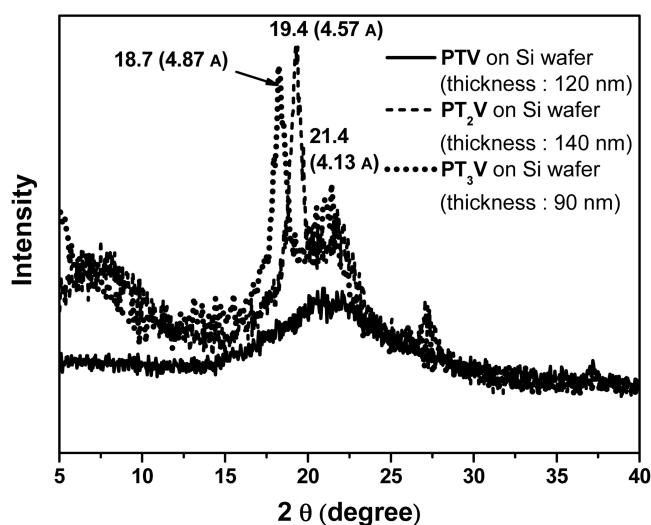
Figure 11. X-ray diffractograms of PT_mV films on Si wafer (001).[55]
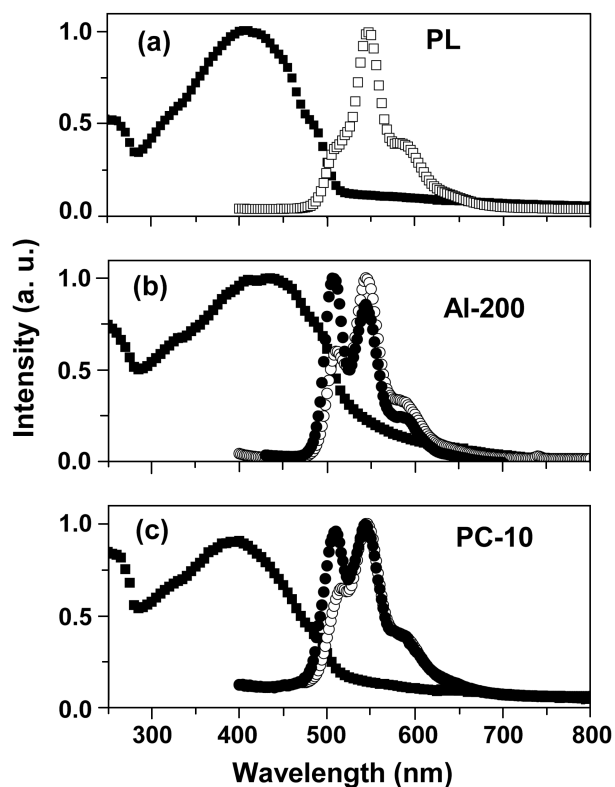
Figure 12. Comparison of UV-vis absorption and photolumines-cence (PL) spectra. ■ : UV-vis absorption spectra ((a): bulk PPV film; (b): PPV nanotubes (AL-200) in the methanol suspension; (c): PPV nanorods (PC-10) in methanol suspension), □ : PL spectrum of bulk film, ● : PL spectra of nanotubes and nanorods in filter membranes, ○ : PL spectra of nanotubes and nanorods suspended in methanol (All the PL spectra were obtained at the excitation wavelength of 350 nm).[2]

samples prepared in different dimensions.[2] The spectra of nano tubes and wires were obtained for methanol suspen-sion, whereas the spectra of the bulk sample were taken for a film 430 nm thick. The λ_{max} value of the absorption spectra is 410 nm regardless the dimension of the sample. The peak
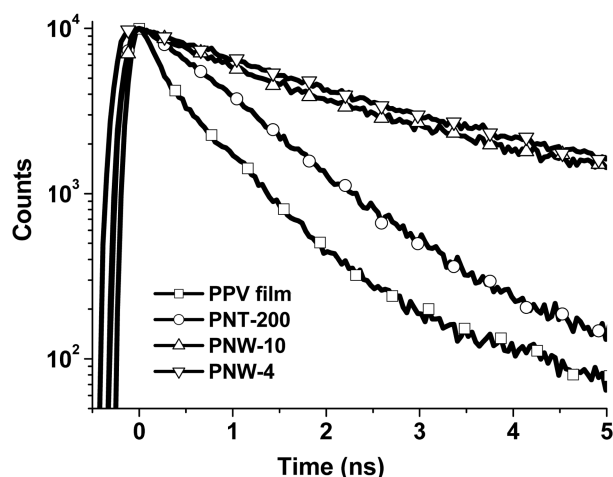

Figure 13. PL decays of PPV nano film, tubes and wires.[66]

is ascribed to the $\pi \rightarrow \pi^*$ transition. One noticeable differ-ence among the spectra can be found in the tail part of the spectra: the nano PPV samples suspended in methanol reveal much longer tail extending to more than 700 nm, while the spectrum of the bulk film reaches the baseline at about 500 nm. Moreover, peak broadening also was observ-ed for the methanol suspensions of nano PPV samples. The similar phenomenon was observed by Wu *et al.*[64,65] for MEh-PPV prepared in mesoporous silica. This can be explained by the inhomogeneous environment around the PPV mole-cules in the nano samples.

We, however, observe much more distinct differences in their fluorescence spectra: all of them exhibit three peaks at 510, 545, and 585 nm with vibronic details. The three peaks correspond to $S_1 \rightarrow S_0$ (0 → 0), (0 → 1), and (0 → 2) transitions, respectively. Although the nano samples in the membranes show less intensity for the peak at 510 nm when compared to the central major peak at 545 nm, when they were dispersed in methanol the intensity of the peak in the shortest emission wavelength grows sharply. The PPV chains in isolated nanotubes and wires in methanol suspension are expected to be involved in much reduced interactions with solid environment or neighboring chains. This would give less chance for the high energy excitons to migrate to lower energy states before they become involved in a radiative or nonradiative decay. This, in turn, will give rise to an enhanc-ed intensity for the 0 → 0 transition as we observed.[66]

In addition, we found that fluorescence decay behavior of PPV samples strongly depends on their dimension. Figure 13[66] compares time-resolved fluorescence decay of PPV samples of varying dimensions; bulk film (430 nm thick), nanotubes of outer diameter of 285 nm having the thickness of 28 nm, nanowires of diameter of 31 nm and nanofibers. And it is clear that the thicker the sample, the faster the decay time becomes. Moreover, fluorescence quantum effi-ciency steadily increases from 12% for the bulk film to 24.7% for the nanofiber. The quantum efficiency values of the nanotube and nanowire were 14.8 and 18.2%, respec-tively. The longer fluorescence lifetime and less interchain
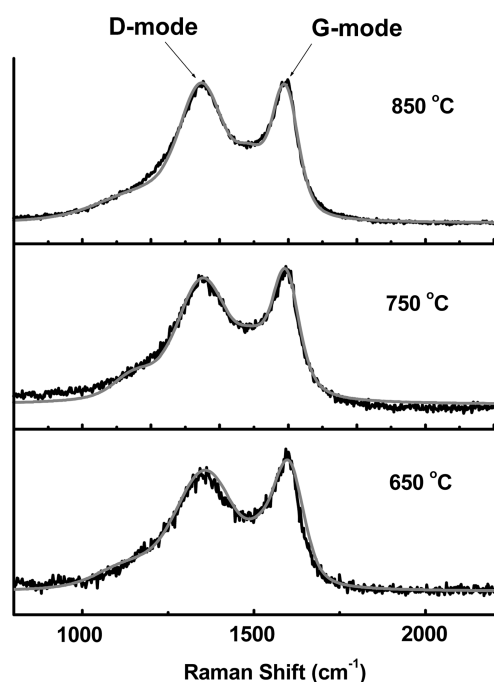
Table 2. Comparison of fluorescence decay time of PPV film, nanotubes and nanowires[66]

	τ_1	τ_2	τ_3
	Decay time (ratio) (ns)	Decay time (ratio) (ns)	Decay time (ratio) (ns)
Bulk film	0.087 (0.83)	0.48 (0.17)	–
PNT-200[a]	0.31 (0.86)	0.88 (0.14)	–
PNW-10[b]	0.17 (0.46)	0.75 (0.33)	2.4 (0.21)
PNW-4[c]	0.27 (0.36)	0.92 (0.46)	2.2 (0.18)

[a]Nanotube with O.D. of 285 nm and thickness of 28 nm. [b]Nanotube with O.D. of 31 nm and thickness of 10 nm. [c]Nanofiber with diameter of 4 nm

Table 3. Graphitic cluster diameter (L_a) of in-plane correlation length[69]

	A (G) / A (D)[a]	Graphitic Cluster Diameter (La) (nm)
CPNW-4[b]	0.75	3.3
CPNW-20[c]	0.66	2.9
CPNT-100[d]	0.64	2.8
CPNT-200[e]	0.60	2.6

[a]Ratio of the intensities between the G and D modes. [b]Carbonized PPV nanowire of PNW-4 in Table 2. [c]Cabonized of PPV nanowire of diameter of 25 nm. [d]Carbonized PPV nanotube with O.D. of 120 nm and wall thickness of 30 nm. [e]Carbonized PPV nanotube of PNT-280 in Table 2.

contacts in the nano samples improve the fluorescence efficiency. Wu *et al.*[65] observed that fluorescence decay of MEh-PPV in dilute solutions is much longer than that of bulk sample. Heller *et al.*[67] also learned that fluorescence lifetime of oligomer PPV was very much lengthened when blended with PMMA. Coincidentally, the slow decay time (τ_3 in Table 2) of about 2 ns for the nanowire and nanofiber is very similar to those reported by Wu *et al.*[65] and Heller *et al.*[67] for the systems described above.

Preparation of Carbonized PPV Nanotubes and Field Emission Properties. Ueno and Yoshino[68] demonstrated earlier that PPV films could be readily converted to graphitic carbons by thermal carbonization. We[69] carbonized PPV nanotubes (OD: 285 nm; thickness: 28 nm) at three different temperatures and their degree of carbonization was studied by the Raman spectroscopy (Figure 14). The spectra show two distinct peaks at 1350 and 1590 cm^{-1}. The former is characteristic to defective graphite structures and called D-mode, whereas the latter is from well-structured graphitic

structure and called G-mode.[70] From the relative intensity or area of the peaks, one can estimate the average graphitic cluster diameter (L_a) or in-plane correlation length.[69] Table 3 summarizes pertinent parameters together with electrical conductivities of the carbonized tubes. The table tells us that the La value and electrical conductivity both increase with increasing carbonization temperature. The L_a value reached 2.6 nm at 850 °C, which indicates that about 8 graphitic rings are in one cluster. The electrical conductivity of 170 Scm^{-1} obtained for the sample carbonized at 850 °C is somewhat higher than that reported for the carbonized PPV bulk films.

As discussed above, morphology of PPV films obtained by CVDP greatly depends on the nature of substrates. Figure 15[71] compares the electrical conductivity of two carbonized films prepared from PPV thin films obtained on the surface of Si(001) and quartz. It is seen that the carbon film formed at 850 °C on the Si(001) surface is consistently higher than that formed on the quartz surface. In fact, the room temperature conductivity ($\sigma \sim 450$ Scm^{-1}) of the former is comparable to that of the carbon obtained at 2000 °C from bulk PPV prepared by Wessling-Zimmerman method.[68]

This observation clearly demonstrates that graphitization process is highly controlled by the morphology of the starting polymer. Thinner thickness of the nanofilms also

Figure 14. Comparison of Raman spectra of PPV nanotubes carbonized at three different temperatures.[69]
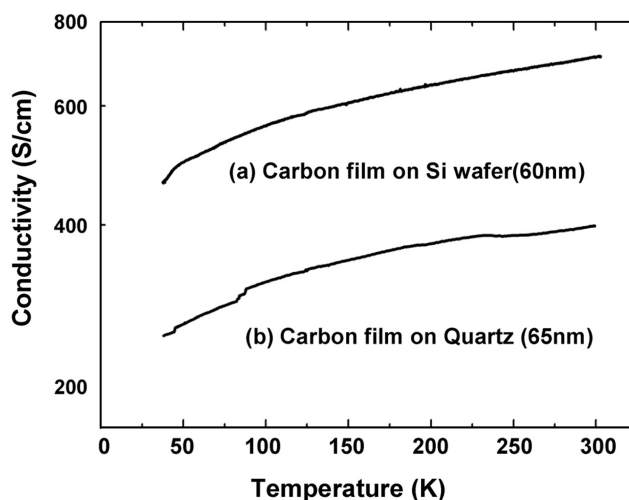
Figure 15. Comparison of electrical conductivities of two carbonized films prepared from PPV thin films obtained at 850° C on the surface of Si(001) and quartz.[71]
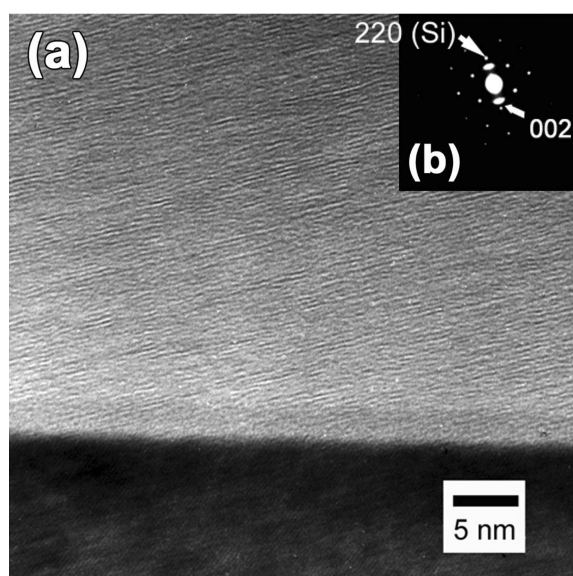
Figure 16. (a) Cross sectional TEM image and (b) electron diffraction of a carbon film on Si wafer.[71]

Figure 17. (a) Preparation procedure of graphitic carbon nanotubes embedded with Au nanoparticles (I: first CVD polymerization of PPV, II: deposition of Au nanopariticles, III: second CVD polymerization of PPV and IV: Carbonization), (b) TEM images of the Au-CPNTs (bottom left and right), (c) SEM images of the aligned Au-CPNTs after removal of alumina membrane.[7]

must have favored a higher degree of graphatization due to more efficient thermal flux. Figure 16[71] shows the TEM image of the graphitic carbon film together with its electron diffraction pattern; we can clearly identify the graphitic layered structure with layer distance being 3.4 Å. The electron diffraction also shows a sharp crystalline scattering confirming well-developed graphitic structure.

Field Emission of Carbonized PPV Nanotubes. In 1995 Smally *et al.*[72] and de Heer *et al.*[73] reported their successful fabrication of field emission devices utilizing carbon nanotubes. This stimulated intensive researches on the field emission properties of various carbon nanotubes. One of the most attractive motives for such research interests lies in the possibility of using the carbon nanotubes as electron guns, *i.e.*, cathode, in flat panel displays including TVs. Although the field emission property strongly depends on the detailed structure of carbon nanotubes, turn- on applied field was reported to be 2-5 V/μm. It is a generally accepted convention in this area of research that the electrical field at the current density of 10 μA/cm^2 is taken as turn-on applied field.

The field amplification factor (β) estimated by applying the Fowler-Nordheim theory[74] is 2,000-10,000. The theory was originally developed to interpret the emission of cold electrons from metals under strong applied field. Among many variables, geometric shape, work function and surroundings of emitter are the most critical factors controlling the β value. The large aspect ratio is another factor for elevated β values.

Carbon nanotubes have many desirable properties for improved field emission: excellent electrical and thermal conductivity, mechanical strength, high aspect ratio and not too high work function. In spite of these attractive features of carbon nanotubes, there is a couple of technological problems to be resolved before they can be practically

utilized. Their easy production and reproducible alignment in large scale are the most pressing issues.

Instead of carbon nanotubes, graphitic carbonized PPV nanotubes prepared in an alumina membrane and similar nanotubes embedded with gold nanoparticles were employed by us[7] in fabricating field emitting devices (Figure 17(a), (b), and (c)). As shown in Figure 17(a) the nanotubes are a little deformed, but extremely well aligned as expected. Figure 17(b) shows the schematic presentation of the device together with relevant information. Figure 18 exhibits a TEM image of a nanotube embedded with 3 atom % of Au

Figure 18. TEM images of Au- CPNTs (Inset: electron diffraction pattern).

Figure 19. Voltage dependence of the current with (□ : bilayer nanotube I, ○ : bilayer nanotube II) and without light (■ : bilayer nanotube I, ● : bilayer nanotube II). The thickness of the carbon layer was fixrd at 3 nm and the thickness of bilayer nanotube I, II were 4 nm and 18 nm, respectively. Inset: light intensity dependence of photocurrent of bilayer nanotube II at 1.0 V.[79]

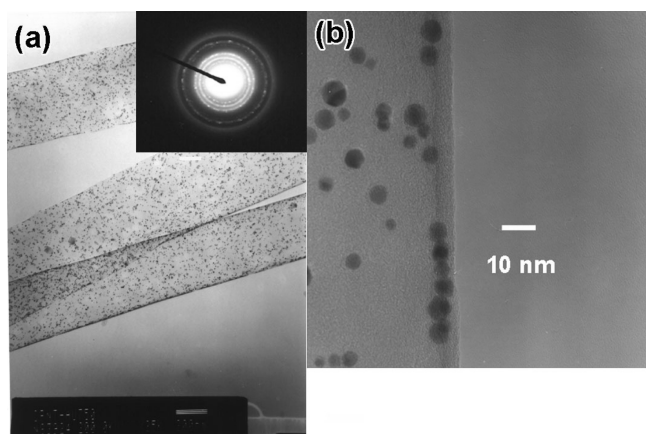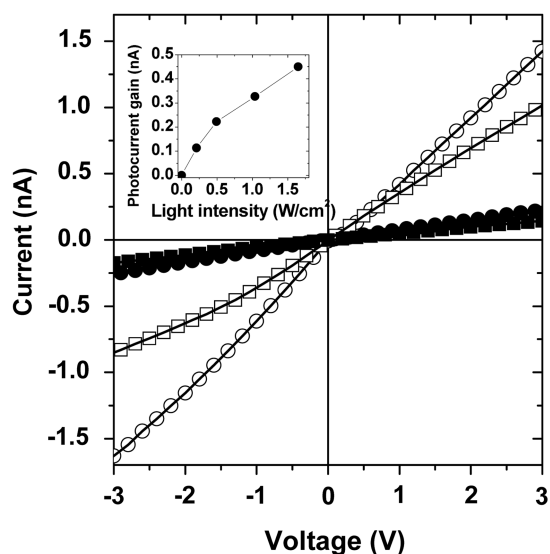particles of 5.3 ± 1.1 nm. The field emission characteristics of the two devices are summarized in Table 4. Several important findings are noted: 1) the performance of the two devices is comparable to or better than those reported for carbon nanotube-based devices, 2) the work function and turn-on field are reduced significantly by the presence of Au-nanoparticles, and 3) the field amplification factor was doubled when Au-nanoparticles were embedded. The reduction in the work function of the nanotubes by Au nanoparticles was confirmed by XPS studies,[7] which is an interesting observation that can be controversial. It, however, is pointed out that a similar phenomenon was reported earlier.[75]

According to Figure 17(a), there are chinks between the nanotubes. Bonard *et al.*[76] demonstrated that separation between the carbon nanotubes are very important to elevate the field amplification factor by reducing the screening effect. The presence of chinks as shown in Figure 17(a), can mitigate the screening effect to a certain extent. When the tubes are in touch or too close to each other, emitted electrons can stand in other electrons' pathways, which, in turn, reduces the amplification factor of the device.

Photoconductivity of Bilayer Nanotubes Consisting of PPV and Carbonized PPV Layers. PPV is photoconducting[77-79] as many other conjugated polymers.[80-82] Its photoconductivity, however, is relatively small because of low mobility of carriers, especially of electrons. In contrast, regioregularly substituted poly(3-alkyl)thiophenes reveal high photoconductivity,[83-86] which is believed to be high enough for practical applications. Photovoltaic applications of polyconjugated polymer are attracting ever increasing

interests. Blending of polyconjugated polymers with carbon-60 is a popular approach being taken to improve the solar energy conversion efficiency.[86-89] But discrete distribution in the matrix and relatively low electrical conductivity of C-60 limit the achievable efficiency in solar energy conversion, although graphitic carbons are known to be excellent electron acceptors and negative charge (e⁻) transporters.

The CVDP method provides us with an easy approach to the preparation of bilayered nanotubes and nanofilms consisting of carbon and PPV layers.[79] Preparation and carbonization of PPV nanotubes in alumina membranes followed by the second CVDP of PPV provids desired bilayered structures. After the membrane host was removed by dissolving it in a dilute alkali solution, the individual bilayer nanotubes were isolated and washed. Figure 19 compares the photoconductivity of two different bilayer nanotubes before and after being exposed to a xenon lamp. In the dark, the carbonized nanotube itself and the bilayer tubes exhibit the same electrical conductance, which is ascribed to the flow of charge carriers through the carbon layer. The bilayer devices, however, revealed an enhanced conductance under illumination, although the devices made only of carbonized PPV nanotubes did not. The minimum external quantum efficiencies of 4 and 6% were estimated respectively for device I and II (Figure 20). The values are three orders of magnitude higher than that of PPV films and comparable to those reported for PPV composites[90] and heterojunction film devices.[91] Two major reasons were proposed to be responsible for the high efficiencies: the longer photoluminescence lifetime of nanothin PPV tubes and efficient electron transfer to the carbon layer from the PPV layer after the excitons formed in the PPV layer by light absorption are separated by the carbon interface in contact. It is believed that the

Table 4. Field emission characteristics of the two devices[7]

	CPNT	Au-CPNT
Au content (atom%)	0.0	3.0
V_{TO} (V/μm)[a]	3.1	2.1
Φ (eV)[b]	5.51	5.02
β^c	4,910	11,500

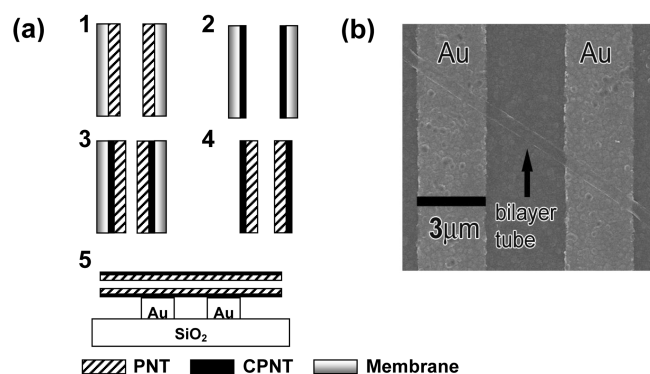[a]Turn-on electric field. [b]Workfunction. [c]Field amplication factor

Figure 20. (a) Preparation of bilayer nanotubes. 1: CVDP of PPV to form PNT, 2: carbonization of PNT to CPNT, 3: second CVDP of PPV, 4: removal of alumina membrane, 5: deposition of the CPNT/PNT bilayer nanotube on patterned Au electrodes. (b) SEM image of a bilayer nanotube on the patterned Au electrodes.[79]
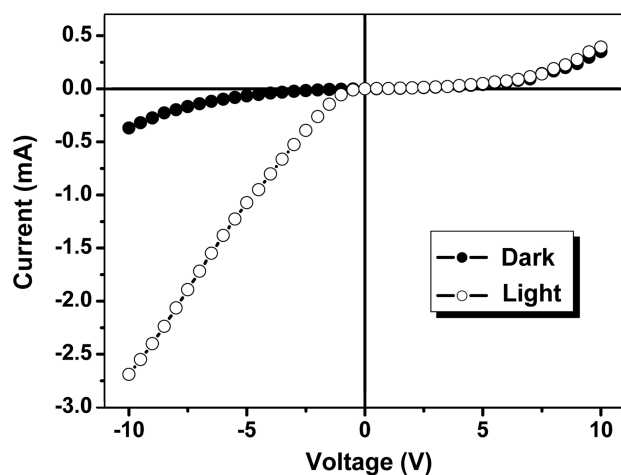

Figure 21. Voltage dependence of the current with (○) and without (●) light of bilayer device (Light source : Xe lamp).[93]

thickness of the PPV layer should not be much thicker than 10 nm, because the exciton diffusion length in PPV was claimed to be about 7-10 nm.[92]

Two layer photoconducting nanodevices can be more easily constructed in thin film forms by depositing PPV nanofilms (40 nm thick) on the carbonized (1000 °C) PPV substrate (60 nm thick). The carbon layer and a thin (30 nm) gold film deposited on the PPV layer were utilized as electrodes. Figure 21 shows the current (I) – applied field (V) curves for two bilayer devices in film form.[93] The external quantum efficiency of the bilayer film device is significantly higher (*ca*. 11.3%) than for the above-meationed bilayer tube devices, which is believed to be the result of a better contact between the active layer and the electrodes. The asymmetrical rectification, however, is observed in the device for the voltage beyond −0.7 V and +5.5 V with the I-V characteristics showing Ohmic contact. This asymmetrical rectification behavior is often observed in the devices consisting of two different electrodes (Eg. ITO/Polymer/Al).[94] It is caused by the difference of workfunctions of two electrodes.
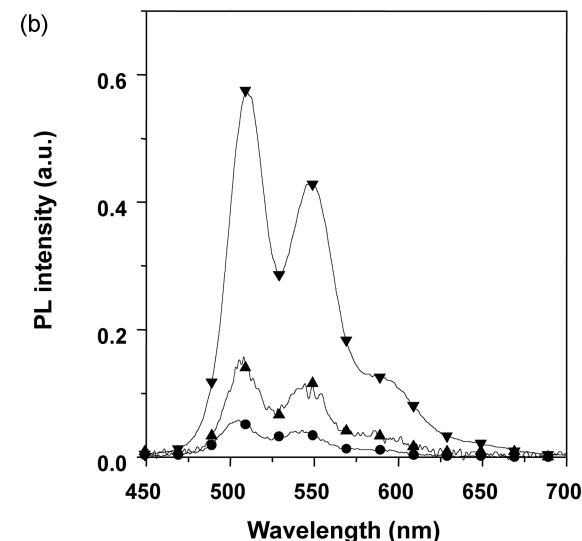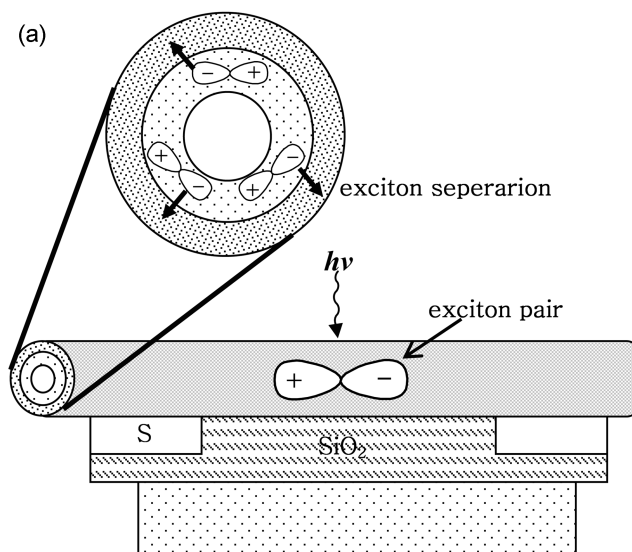
Figure 22. (a) Diagram of exciton separation by the contacting carbon layer and (b) comparison of PL spectra of PPV and the bilayer tubes (▼ : PPV, ▲ : bilayer nanotube I, ● : bilayer nanotube II)[79].

The high efficiency implies that the simple devices like the present bilayer ones can be useful in photoswitching and also possibly in photovoltaic applications. Another advantage of the present approach is the easy fabrication of flexible devices on plastic substrates.

Exciton separation by the contacting carbon layer is schematically depicted in Figure 22 that compares PL spectra of PPV and those of the two bilayer tubes mentioned above. It is clear that contact of the PPV layer with the carbon layer efficiently quenches the PL of the former.

$$PPV \xrightarrow[\text{exciton formation}]{h\nu} \begin{array}{c} h^+ \text{---} e^- \\ \text{excitons in PPV} \end{array}$$

$$\xrightarrow[\text{exciton seperation}]{carbon} \overset{+}{h} + e^-$$
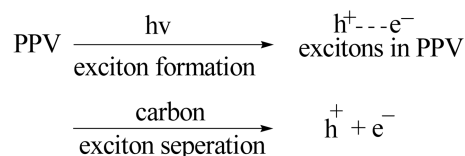
Conclusion and Perspective

At the present moment, poly(*p*-xylylene)s, or PPXs, are the only commercial polymers being produced by the CVDP method.[95] But, as has been described and discussed in this article, the CVDP method can be very useful for the preparation of a wide variety of insoluble poly(arylenevinylene)s in desired dimensions and shapes. In addition to poly(arylenevinylene)s, poly(1,4-naphthalene)s,[96] polyimides,[97] and poly(tetrafluoroethylene)[98] also can be prepared by CVDP.[99] Therefore, it appears that application of CVDP is not limited to poly(arylenevinylene)s.

There, however, remain many scientific questions to be answered : 1) The reaction mechanism requires much more and deeper studies. Although the precursor polymers are expected to be soluble in organic solvents, they usually are only slightly soluble, which suggests that unidentified crosslinking reactions may occur during polymerization. It seems to be genuinely possible that precursor polymer chains undergo secondary reactions with activated monomer molecules as leading to the formation of crosslinked structures. 2) Molecular weights of CVDP polymers are largely unknown, because precursors and the final polymers are not soluble. According to UV-vis absorption characteristics, their average conjugation length probably should be higher than penta or hexamers. 3) Although it has not been reported, we[100] observe that PPV samples prepared by CVDP show rather strong epr signals suggesting that some of growing chain radicals are trapped during polymerization. This could be one of the reasons why PPV films prepared by the CVDP method exhibit poor photo- and electroluminescence when compared with those prepared by other conventional methods. The presence of free radical impurities are known to quench luminescence.[101] 4) Kinetic modeling of thin film growth is necessary to understand and control the film formation. It was claimed that the so-called chemisorption model[102] fits the experimental data very well in the case of CVDP of PPX. 5) To the best of our knowledge thermodynamics study on CVDP of poly(arylenevinylene)s is non-existent. Although collection of thermodynamics quantities is expected to be rather difficult due to the heterogeneous nature of CVDP, thermodynamic data are essential in understanding the polymerization mechanism and controlling polymerization reactions. Thermodynamic information on each elementary reaction is essential in establishing the structure-reactivity reactions of monomers and reactive intermediates. 6) And the last but not the least, there is not a general, easy guideline to find the optimum polymerization condition such as pyrolysis or activation temperature of monomers and substrate or polymerization temperature. In short, it is emphasized that CVDP of poly(arylenevinylene)s is in its infant stage and requires much more basic studies to make the process more practically adoptable. In spite of much lacking in scientific understanding of CVDP, it is expected that the method will continue to attract more attention in polymer community, especially related to nanoscience and nanotechnology. Fabrication of large device, however, can be somewhat problematic.

References

1. Friend, R. H.; Gymer, R. W.; Holmes, A. B.; Burroughes, J. H.; Marks, R. N.; Taliani, C.; Bradley, D. D. C.; Dos Santos, D. A.; Brédas, J. L.; Lögdlund, M.; Salaneck, W. R. *Nature* **1999**, *397*, 121.
2. Kim, K.; Jin, J.-I. *Nano Lett.* **2001**, *1*, 631.
3. Berlin, A.; Zotti, G.; Zecchin, S.; Schiavon, G. *Macro. Chem. Phys.* **2002**, *203*, 1228.
4. Cavallaro, S.; Colligiani, A.; Fotis, C. G. *J. Therm. Anal. Calorim.* **1995**, *44*, 269.
5. Joo, J.; Lee, S. J.; Park, D. H.; Lee, J. Y.; Lee, T. J.; Seo, S. H.; Lee, C. *J. Electrochem. Solid- State Lett.* **2005**, *8*, H39.
6. (a) Shim, H.-K.; Jin, J.-I.; Lenz, R. W. *Makromol. Chem.* **1989**, *190*, 389. (b) Murase, I.; Ohnishi, T.; Noguchi, T.; Hirooka, M. *Polym. Commun.* **1987**, *28*, 229. (c) Xie, H.-Q.; Liu, C.-M.; Guo, J.-S. *Eur. Polym. J.* **1996**, *32*, 1131.
7. Kim, K.; Lee, S. H.; Yi, W.; Kim, J.; Choi, J. W.; Park, Y. S.; Jin, J.-I. *Adv. Mater.* **2003**, *15*, 1618.
8. Yanagishita, H.; Nakane, T.; Nozoye, h.; Yoshitome, H. *J. Appl. Polym. Sci.* **1993**, *49*, 565.
9. (a) Cheng, S. Z. D.; Wu, Z. Q.; Wunderlich, B. *Macromolecules* **1987**, *20*, 2802. (b) Yang, Y.; Pei, Q. *J. Appl. Phys.* **1996**, *79*, 934.
10. Burroughes, J. H.; Bradley, D. D. C.; Brown, A. R.; Marks, R. N.; Mackay, K.; Friend, R. H.; Burn, P. L.; Holmes, A. B. *Nature* **1990**, *347*, 539.
11. Bjørnholm, T.; Hassenkam, T.; Greve, D. R.; McCullough, R. D.; Jayaraman, M.; Savoy, S. M.; Jones, C. E.; McDevitt, J. T. *Adv. Mater.* **1999**, *11*, 1218.
12. Yang, Y.; Pei, Q. *J. Appl. Phys.* **1996**, *79*, 934.
13. Zhu, W.; Mo, Y.; Yuan, M.; Yang, W.; Cao, Y. *Appl. Phys. Lett.* **2002**, *80*, 2045.
14. Yang, H. C.; Shin, T. J.; Yang, L.; Cho, K.; Ryu, C. Y.; Bao, Z. N. *Adv. Funt. Mater.* **2005**, *15*, 671.
15. Hoshino, S.; Yoshida, M.; Uemura, S.; Takada, N.; Toshihide, K.; Yase, K. *J. Appl. Phys.* **2004**, *95*, 5088.
16. Kang, J.-G.; Kim, T.-J.; Park, C.; Woo, L. S.; Kim, I. T. *Bull. Korean Chem. Soc.* **2004**, *25*, 704.
17. Nam, N. P. H.; Prasad, V.; Cha, S. W.; Lee, D. W.; Jin, J.-I. *Bull. Korean Chem. Soc.* **2002**, *23*, 1470.
18. Yoshino, K.; Takahashi, H.; Muro, K.; Ohmori, Y. *J. Appl. Phys.* **1991**, *70*, 5035.
19. Heywang, G.; Jonas, F. *Adv. Mater.* **1992**, *4*, 116.
20. Jonas, F.; Krafft, W.; Muys, B. *Macromol. Symp.* **1995**, *100*, 169.
21. (a) Friend, R. H.; Gymer, R. W.; Holmes, A. B.; Burroughes, J. H.; Marks, R. N.; Taliani, C.; Bradley, D. D. C.; Dos Santos, D. A.; Brédas, J. L.; Lögdlund, M.; Salaneck, W. R. *Nature* **1999**, *397*, 121. (b) Kim, J. H.; Lee, H. *Bull. Korean Chem. Soc.* **2004**, *25*, 652. (c) Ko, W. S.; Jung, B.-J.; Jo, N. S.; Shim, H.-K. *Bull. Korean Chem. Soc.* **2002**, *23*, 1235. (d) Kim, Y.-H.; Bark, K.-M.; Kwon, S.-K. *Bull. Korean Chem. Soc.* **2002**, *22*, 975. (e) Jin, Y.; Kim, J.; Song, S.; Park, S. H.; Lee, K.; Suh, H. *Bull. Korean Chem. Soc.* **2005**, *26*, 855.
22. Holmes, A. B.; Grimsdale, A. C.; Kraft, A. *Angew. Chem. Int. Ed.* **1998**, *37*, 402.
23. (a) Wessling, R. A.; Zimmerman, R. G. *U.S. Pat.* **1968**, *3*, 401,152. (b) Wessling, R. A.; Zimmerman, R. G. *U.S. Pat.* **1970**, *3*, 532,643.
24. Wessling, R. A. *J. Polym. Sci. Polym. Symp.* **1985**, *72*, 55.
25. Cho, B. R. *Prog. Polym. Sci.* **2002**, *27*, 307.
26. Conticello, V. P.; Gin, D. L.; Grubbs, R. H. *J. Am. Chem. Soc.* **1992**, *114*, 9708.

27. Pu, L.; Wagaman, M. W.; Grubbs, R. H. *Macromolecules* **1996**, *29*, 1138.
28. Miao, Y. J.; Bazan, G. C. *J. Am. Chem. Soc.* **1994**, *116*, 9379.
29. Denton, F. R.; Lahti, P. M. In *Photonic Polymer Systems-Fundamentals, Methods, and Applications*; ed. by Wise, D. L.; Wnek, G. E.; Trantolo, D. J.; Cooper, T. M.; Gresser, J. D., Eds.; Marcel Dekker Inc.: New York, 1998; Chapter 3.
30. Starings, E. G.; Braun, J. D.; Rikken, G. L. J. A.; Demandt, R. J. C. E.; Kessener, Y. A. R. R.; Bouwmans, M.; Broer, D. *Synth. Met.* **1994**, *67*, 71.
31. Greiner, A.; Schäfer, O.; Pommerehne, J.; Guss, W.; Vestweber, H.; Wendorff, J. H.; Tak, H. Y.; Bässler, H.; Schmidt, C.; Lüssem, G.; Schartel, B.; Stümpflen, V.; Spiess, H. W.; Möller, C.; Spiegel, S. *Synth. Met.* **1996**, *82*, 1.
32. Iwatsuki, S.; Kubo, M.; Kumeuchi, T. *Chem. Lett.* **1991**, 1031.
33. (a) Schäfer, O.; Greiner, A. Unpublished results but cited in ref. 29. (b) Li, A.-K.; Janarthanan, N.; Hsu, C.-S. *Polym. Bull.* **2000**, *45*, 129.
34. Errede, L. A.; Szware, M. *Quart. Rev. Chem. Soc.* **1959**, *12*, 301.
35. Gorham, W. F. *J. Polym. Sci.* **1966**, *4*, 3027.
36. Gorham, W. F. *U.S. Pat.* **1966**, *3*, 288,728.
37. Lee, C. *J. Macromol. Sci. Rev. Macromol. Chem.* **1977-1978**, *C16*, 79.
38. Surendran, G.; Gazicki, M.; James, W. J.; Yasuda, H. *J. Polym. Chem. Ed.* **1987**, *25*, 1481.
39. Greiner, A.; Mung, A.; Schäfer, U.; Simon, P. *Acta Polym.* **1997**, *48*, 1.
40. Liu, A. P.; Fletcher, D. A. *Nano Lett.* **2005**, *5*, 625.
41. Shklover, V. *Chem. Mater.* **2005**, *17*, 608.
42. Rothemund, P. W. K.; Ekani-Nkodo, A.; Papadakis, N.; Kumar, A.; Fygenson, D. K.; Winfree, E. *J. Am. Chem. Soc.* **2004**, *126*, 16344.
43. Cheng, W. L.; Dong, S. J.; Wang, E. K. *J. Phys. Chem. B* **2004**, *108*, 19146.
44. Cheng, J. Y.; Mayes, A. M.; Ross, C. A. *Nat. Mater.* **2004**, *3*, 823.
45. Cho, J.; Char, K.; Hong, J. D.; Lee, K. B. *Adv. Mater.* **2001**, *13*, 1076.
46. Jang, J.; Oh, J. H. *Chem. Commun.* **2004**, 882.
47. Fu, M.; Chen, F.; Zhang, J.; Shi, G. *J. Mater. Chem.* **2002**, *12*, 2331.
48. Martin, C. R. *Science* **1994**, *266*, 1961.
49. Smith, R. C.; Fisher, W. M.; Gin, D. L. *J. Am. Chem. Soc.* **1997**, *119*, 4092.
50. Jang, J.; Yoon, H. *Chem. Commun.* **2003**, 720.
51. Zhang, Z.; Wei, Z.; War, M. *Macromolecules* **2002**, *35*, 5937.
52. Guo, L.; Wu, Z.; Liang, Y. *Chem. Commun.* **2004**, 1664.
53. Tung, N. T.; Yu, Y. J.; Kim, K.; Joo, S. H.; Park, Y.; Jin, J.-I. *J. Polym. Sci. Pol. Chem.* **2005**, *43*, 742.
54. Lee, K.-R. *MS thesis*; Chemistry Department, Korea University, Seoul, Korea, Feb. 2004.
55. Joo, S.-H. *Ph. D. thesis*; Chemistry Department, Korea University, Seoul, Korea, Feb. 2005.
56. Lee, K.-R.; Jeong, S.-H.; Kim, K.; Jin, J.-I. *Macromol. Symp.* in press.
57. Park, J.-S. *MS thesis*; Chemistry Department, Korea University, Seoul, Korea, Feb. 2005.
58. Weitzel, H. P.; Bohnen, A.; Müllen, F. *Makromol. Chem.* **1990**, *191*, 2815.
59. Vaeth, K. M.; Jensen, K. F. *Adv. Mater.* **1997**, *9*, 490.
60. (a) Vaeth, K. M.; Jensen, K. F. *Macromolecules* **2000**, *33*, 5336. (b) Vaeth, K. M.; Jensen, K. F. *Macromolecules* **1998**, *31*, 6789.
61. Chen, D.; Winokur, M. J.; Masse, M. A.; Karasz, F. E. *Polymer* **1992**, *33*, 3116.
62. Kim, K.; Jung, M. Y.; Zhong, G. L.; Jin, J.-I.; Kim, T. Y.; Ahn, D. J. *Synth. Met.* **2004**, *144*, 7.
63. Kim, K.; Jin, J.-I. Unpublished results.
64. Nguyen, T. Q.; Wu, J.; Tolbert, S. H.; Schwartz, B. J. S. *Adv.*

65. Wu, J.; Gross, A. F.; Tolbert, S. H. *J. Phys. Chem. B* **1999**, *103*, 2374.
66. Kim, K.; Jeoung, S. C.; Lee, J.; Hyeon, T.; Jin, J.-I. *Macromol. Symp.* **2003**, *201*, 119.
67. Heller, C. M.; Campbell, I. H.; Laurich, B. K.; Smith, D. L.; Bradley, D. D. C.; Burn, P. L.; Ferraris, J. P.; Mullen, K. *Phys. Rev. B: Condens. Matter.* **1996**, *54*, 5516.
68. Ueno, H.; Yoshino, K. *Phys. Rev. B: Condens. Matter.* **1986**, *34*, 7158.
69. Kim, K. *Ph. D. thesis*; Chemistry Department, Korea University, Seoul, Korea, Feb. 2003.
70. Ferrari, A. C.; Robertson, J. *Phys. Rev. B : Condens. Matter* **2000**, *61*, 14095.
71. Kim, K.; Zhong, G. L.; Jin, J.-I. *Macromol. Symp.* **2003**, *195*, 217.
72. Dai, H. J.; Hafner, J. H.; Rinzler, A. G.; Colbert, D. T.; Smallery, R. E. *Nature* **1996**, *384*, 147.
73. de Heer, W. A.; Chatelain, A.; Ugarte, D. *Science* **1995**, *270*, 1179.
74. Fowler, R. H.; Nordheim, L. *Proc. Roy. Soc. London* **1928**, *A119*, 173.
75. Wadhawan, A.; Stallcup, R. E.; Perez, J. M. *Appl. Phys. Lett.* **2001**, *78*, 208.
76. Bonard, J. M.; Weiss, N.; Kind, H.; Stockli, T.; Forro, L.; Kern, K.; Chatelain, A. *Adv. Mater.* **2001**, *13*, 184.
77. Antoniadis, H.; Hsieh, B. R.; Abkowitz, M. A.; Stolka, M.; Jenekhe, S. A. *Abst. Am. Soc.* **1993**, *206*, 105.
78. Park, H.; Choi, Y. S.; Park, Y. W.; Park, C. K.; Jin, J.-I.; Kaiser, G.; Roth, S. *Synth. Met.* **1997**, *84*, 965.
79. Kim, K.; Kim, B. H.; Joo, S.-H.; Park, J.-S.; Joo, J.; Jin, J.-I. *Adv. Mater.* **2005**, *17*, 464.
80. (a) Song, M. Y.; Kim, J. K.; Kim, K. J.; Kim, D. Y. *Synth. Met.* **2003**, *137*, 1387. (b) McDonald, S. A.; Konstantatos, G.; Zhang, S. G.; Cyr, P. W.; Klem, E. J. D.; Levina, L.; Sargent, E. H. *Nat. Mater.* **2005**, *4*, 138.
81. Bakulin, A. A.; Elizarov, S. G.; Khodarev, A.; Martyanov, D. S.; Golovnin, I.; Paraschuk, D. Y.; Triebel, M. M.; Tolstov, I.; Frankevich, E. L.; Arnautov, S. A.; Nechvolodova, E. M. *Synth. Met.* **2004**, *147*, 221.
82. (a) Sohn, Y.; Richter, J.; Ament, J.; Stuckless, J. T. *Appl. Phys. Lett.* **2004**, *84*, 76, (b) Suh, D. J.; Park, O. O.; Ahn, T.; Shim, H. K. *Opt. Mater.* **2003**, *21*, 365.
83. Kroeze, J. E.; Savenije, T. J.; Vermeulen, M. J. W.; Warman, J. M. *J. Phys. Chem. B* **2003**, *107*, 7696.
84. Hartmann, T.; Schrof, W.; Belov, V.; Mohwald, H.; Barth, S.; Van Keuren, E.; Mahrt, R. F. *Phys. Rev. B* **2001**, *64*, 235205.
85. Hwang, I. W.; Song, N. W.; Park, Y. T.; Kim, D.; Kim, Y. R. *Eur. Polym. J.* **1998**, *34*, 335.
86. Yoshino, K.; Yin, X. H.; Morita, S.; Kawai, T.; Zakhidov, A. A. *Solid State. Commun.* **1993**, *85*, 85.
87. Alem, S.; De Bettignies, R.; Nunzi, J. M.; Cariou, M. *Appl. Phys. Lett.* **2004**, *84*, 2178.
88. Gao, J.; Hide, F.; Wang, H. L. *Synth. Met.* **1997**, *84*, 979.
89. Xue, J.; Uchida, S.; Rand, B. P.; Forrest, S. R. *Appl. Phys. Lett.* **2004**, *84*, 3013.
90. Mulazzi, E.; Perego, R.; Aarab, H.; Mihut, L.; Lefrant, S.; Faulques, E.; Wery, J. *Phys. Rev. B* **2004**, *70*, 155206.
91. Ahn, Y. J.; Kang, G. W.; Lee, C. H.; Yeom, I. S.; Jin, S. H. *Synth. Met.* **2003**, *137*, 1447.
92. Stubinger, T.; Brutting, W. *J. Appl. Phys.* **2001**, *90*, 3632.
93. Joo, S.-H.; Jin, J.-I. Unpublished results; In preparation.
94. Sharama, G. D.; Gupta, S. K.; Roy, M. S. *Thin Solid Films* **1998**, *333*, 176.
95. Fortin, J. B.; Lu, T.-M. *Chemical Vapor Deposition Polymerization-The Growth and Properties of Parylene Thin Films*; Kluwer Academic Publishers: New York, U.S.A., 2004.
96. Moore, J. A.; Lang, C.-I.; Lu, T.-M.; Yang, G. R. *Polym. Mater. Sci. Eng.* **1995**, *72*, 437.

97. Strunskus, T.; Grunze, M. In *Polyimids: Fundamental and Applications*; Ghosh, M. K., Mittal, K. L. Eds.; Marcel Dekker: New York, 1996; p 187.
98. Nason, T. C.; Moore, J. A.; Lu, T.-M.; *Appl. Phys. Lett.* **1992**, *60*, 1866.
99. Moore, J. A.; Lang, C.-I.; Lu, T.-M.; Yang, G. R. In *ACS Symposium Series*; 1995, 614, 449, American Chem. Soc, Washington D.C., U.S.A., 1995; p 614, 449.
100.Lee, C.-Y.; Lee, C.-H.; Do, E.-D.; Jin, J.-I. Unpublished results.
101.Buchachenko, A. L.; Khloplyankina, M. S.; Dobryakov, S. N. *Opt. Spectrosc+.* **1967**, *22*, 304.
102.Fortin, J. B.; Lu, T.-M. *Chem. Mater.* **2002**, *14*, 1945.